

# PoSynDA: Multi-Hypothesis Pose Synthesis Domain Adaptation for Robust 3D Human Pose Estimation

Hanbing Liu\*  
liuhb21@mails.tsinghua.edu.cn  
Tsinghua University

Jun-Yan He\*<sup>†</sup>  
leyuan.hjy@alibaba-inc.com  
DAMO Academy, Alibaba Group

Zhi-Qi Cheng\*<sup>†</sup>  
zhiqic@cs.cmu.edu  
Carnegie Mellon University

Wangmeng Xiang  
wangmeng.xwm@alibaba-inc.com  
DAMO Academy, Alibaba Group

Qize Yang  
qize.yqz@alibaba-inc.com  
DAMO Academy, Alibaba Group

Wenhao Chai  
wchai@uw.edu  
University of Washington

Gaoang Wang  
gaoangwang@intl.zju.edu.cn  
Zhejiang University

Xu Bao  
baoxu@email.szu.edu.cn  
DAMO Academy, Alibaba Group

Bin Luo  
luwu.lb@alibaba-inc.com  
DAMO Academy, Alibaba Group

Yifeng Geng  
cangyu.gyf@alibaba-inc.com  
DAMO Academy, Alibaba Group

Xuansong Xie  
xingtong.xxs@taobao.com  
DAMO Academy, Alibaba Group

## ABSTRACT

The current 3D human pose estimators face challenges in adapting to new datasets due to the scarcity of 2D-3D pose pairs in target domain training sets. We present the *Multi-Hypothesis Pose Synthesis Domain Adaptation (PoSynDA)* framework to overcome this issue without extensive target domain annotation. Utilizing a diffusion-centric structure, PoSynDA simulates the 3D pose distribution in the target domain, filling the data diversity gap. By incorporating a multi-hypothesis network, it creates diverse pose hypotheses and aligns them with the target domain. Target-specific source augmentation obtains the target domain distribution data from the source domain by decoupling the scale and position parameters. The teacher-student paradigm and low-rank adaptation further refine the process. PoSynDA demonstrates competitive performance on benchmarks, such as Human3.6M, MPI-INF-3DHP, and 3DPW, even comparable with the target-trained MixSTE model [66]. This work paves the way for the practical application of 3D human pose estimation.<sup>1</sup>

## CCS CONCEPTS

• **Computing methodologies** → **Computer vision; Activity recognition and understanding; Mixture modeling.**

\*Equal contribution, authors are listed in random order

<sup>†</sup>Zhi-Qi Cheng and Jun-Yan He are the corresponding authors

<sup>1</sup>The code is available at <https://github.com/hbing-l/PoSynDA>

Permission to make digital or hard copies of all or part of this work for personal or classroom use is granted without fee provided that copies are not made or distributed for profit or commercial advantage and that copies bear this notice and the full citation on the first page. Copyrights for components of this work owned by others than the author(s) must be honored. Abstracting with credit is permitted. To copy otherwise, or republish, to post on servers or to redistribute to lists, requires prior specific permission and/or a fee. Request permissions from [permissions@acm.org](mailto:permissions@acm.org).

MM '23, October 29–November 3, 2023, Ottawa, ON, Canada

© 2023 Copyright held by the owner/author(s). Publication rights licensed to ACM.

ACM ISBN 979-8-4007-0108-5/23/10...\$15.00

<https://doi.org/10.1145/3581783.3612368>

## KEYWORDS

3D human pose estimation, diffusion model, domain-adaptation, multi-hypothesis, Low-Rank adaptation

## ACM Reference Format:

Hanbing Liu, Jun-Yan He, Zhi-Qi Cheng, Wangmeng Xiang, Qize Yang, Wenhao Chai, Gaoang Wang, Xu Bao, Bin Luo, Yifeng Geng, and Xuansong Xie. 2023. PoSynDA: Multi-Hypothesis Pose Synthesis Domain Adaptation for Robust 3D Human Pose Estimation. In *Proceedings of the 31st ACM International Conference on Multimedia (MM '23)*, October 29–November 3, 2023, Ottawa, ON, Canada. ACM, New York, NY, USA, 10 pages. <https://doi.org/10.1145/3581783.3612368>

## 1 INTRODUCTION

The rise of meta-universes and perception-based entertainment [1, 6–12, 23, 28, 47, 52, 68], has revived the need for advanced 3D Human Pose Estimation (3D HPE) [5, 37, 53, 71–73]. Essential for various real-world applications, 3D HPE deals with the estimation of posture and temporal modeling within a 2D skeleton sequence. Despite significant progress in the field [5, 14, 20, 24, 25, 67], current methodologies often struggle with the complexities arising from a variety of scenes and the wide range of 2D-3D human pose datasets [29]. This, in turn, culminates in a recognizable obstacle in terms of scenario adaptability.

As a result, the challenges of gathering quality 3D HPE data in complex target scenarios and the issues of ill-posed and inaccurate data transformations are the major obstacles. Previous efforts in domain adaptation for 3D HPE have been mainly focused on conventional augmentation schemes [16] and aligning source and target data within the same scale space [4], often resulting in only marginal improvements. Motivated by recent progress in generative models [26], we introduce the *Multi-Hypothesis Pose Synthesis Domain Adaptation (PoSynDA)* framework (Figure 1), focusing on the following five key aspects:

- (1) *Enhanced domain-adaptation* through a generative, target-specific source augmentation, using a multi-hypothesis approach to emulate the target data distribution.

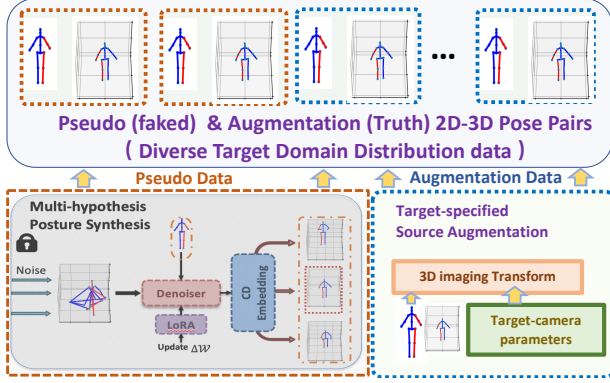


**Figure 1: Overview of Multi-Hypothesis Pose Synthesis.** Multiple viable 3D poses for the target domain are generated using the target’s 2D skeleton. The most accurate hypothesis is selected as the pseudo label. Target-specific source augmentation is applied, aligning generated 2D-3D pose pairs with the target domain’s distribution.

- (2) *Replication of diverse target-domain data* by decoupling the scale factor from domain adaptation, aligning source and target data, and simplifying the underlying distribution.
- (3) *Realistic data distribution* via a multi-hypothesis synthesis generative pipeline, synthesizing pseudo-data and re-projecting it into the target domain.
- (4) *Effective optimization strategy* employing a teacher-student learning paradigm to conduct model training, using teacher network to generate multiple hypotheses and reduce memory usage, while guiding in the generalization ability of student network.
- (5) *Efficient domain adaptation* with low-rank adaptation for large diffusion-based model fine-tuning, optimizing only a minimal set of parameters.

In summary, PoSynDA pioneers a new standard in domain adaptation for 3D pose estimation. Our experiments show that it outperforms existing methods, achieving a 58.2mm MPJPE without using 3D labels from the target domain, comparable with the performance of the target-specific MixSTE model (58.2mm vs. 57.9mm)[66]. This work sets a new benchmark and opens new routes for exploration, extending to various perception-based interactions and meta-universe systems, with the potential to enhance their effectiveness and application range.

## 2 RELATED WORKS

**3D Human Pose Estimation.** 3D Human Pose Estimation (HPE) has attracted considerable attention due to its applicability in various domains [22, 23, 35, 36, 55, 58, 60, 61]. The existing methods are broadly classified into one-step, direct estimation of 3D poses, and two-step, the elevation of 2D keypoints to 3D. Recent innovations include transformer-based approaches such as PoseFormer [70] and MixSTE [66], and GCN [59]. Several works have addressed single-view 3D HPE by generating different hypotheses[30, 39, 51]. In contrast, our PoSynDA method innovatively generates and selects the optimal postures as pseudo-labels during training, enriching the target domain data and adapting to unsupervised scenarios. **Domain Adaptation in 3D HPE.** The challenge of the domain gap in 3D pose estimation requires innovative solutions. Existing

approaches include cross-dataset adaptation, including methods such as BOA [18] and frame-by-frame optimization [65], and augmentation techniques such as MoCap [50] and differentiable pose augmentation [16]. These works mark some progress in matching the data distribution of the target domain. However, our approach goes a step further by uniquely integrating generative techniques to mirror the target data distribution, overcoming significant barriers in domain adaptation for 3D HPE.

**Diffusion Models in Generative Tasks.** Diffusion models such as DDPMs [26] have opened new ways in generative tasks, deconstructing and reconstructing data in various applications, from image and 3D model generation to human motion generation and object detection [49, 54, 62]. This research addresses the inherent challenges of 3D human pose estimation. Uniquely, our method leverages the capabilities of diffusion models to directly synthesize high-fidelity 3D human poses, a distinction that sets it apart from existing methods.

## 3 THE POSYNDA FRAMEWORK

### 3.1 Problem Definition

The problem of unsupervised domain adaptation in 3D human pose estimation seeks to predict accurate 3D human poses across domains like varied lighting, camera perspectives, or motion patterns without labeled target domain data. Acquiring labeled 3D human pose data for all possible scenarios is often prohibitive in terms of cost and time. Consequently, domain adaptation leverages labeled data from a known source domain to enhance the precision of 3D human pose estimations in a target domain lacking labeled data. The aim is to create a model capable of generalizing across domains, thereby bridging the gap between source and target domains.

Formally, we define the source and target domains as  $\mathcal{D}_s = (\mathbf{x}_{2D}^s, \mathbf{y}_{3D}^s)_{i=1}^{n_s}$  and  $\mathcal{D}_t = (\mathbf{x}_{2D}^t)_{i=1}^{n_t}$ , respectively. The source domain  $\mathcal{D}_s$  includes 2D human keypoints  $\mathbf{x}_{2D}^s$  and corresponding 3D coordinates  $\mathbf{y}_{3D}^s$ , while the target domain  $\mathcal{D}_t$  contains only 2D keypoints  $\mathbf{x}_{2D}^t$ . The objective is to design a 3D pose estimator  $\mathcal{P}$  with parameter  $\theta$  to convert 2D keypoints into 3D poses, leading to the following optimization problem:

$$\min_{\theta} \mathcal{L}_{\mathcal{P}}(\mathcal{P}_{\theta}, \mathcal{D}) = \mathcal{L}_{\mathcal{P}}(\mathcal{P}_{\theta}(\mathbf{x}_{2D}), \mathbf{y}_{3D}), \quad (1)$$

where  $\mathcal{D} = (\mathbf{x}_{2D}, \mathbf{y}_{3D})$  consists of paired 2D-3D poses, and the loss function  $\mathcal{L}$  corresponds to the mean square errors (MSE) between predicted 3D poses and ground truths.

We first initialize the 3D pose estimator for the target domain using parameters  $\theta_s$  trained on the source domain. Then, through data augmentation and pseudo-labeling, the model is adapted to the target domain. The augmented data pair  $\mathcal{D}_{aug}$  is used to fine-tune  $\mathcal{P}$ , resulting in the optimization problem:

$$\min_{\theta} \mathcal{L}_{\mathcal{P}}(\mathcal{P}_{\theta}, \mathcal{D}_{aug}; \theta_s) = \mathcal{L}_{\mathcal{P}}(\mathcal{P}_{\theta}(\mathbf{x}_{2D}^{aug}), \mathbf{y}_{3D}^{aug}), \quad (2)$$

where  $\mathcal{D}_{aug} = (\mathbf{x}_{2D}^{aug}, \mathbf{y}_{3D}^{aug})$  includes the augmented source data and pseudo-labeled target data. The ultimate goal is to train a function  $\mathcal{P}$  that accurately predicts the 3D human pose  $\hat{\mathbf{y}}_{3D}^t$  in the target domain, using only the labeled source domain and the unlabeled target domain.

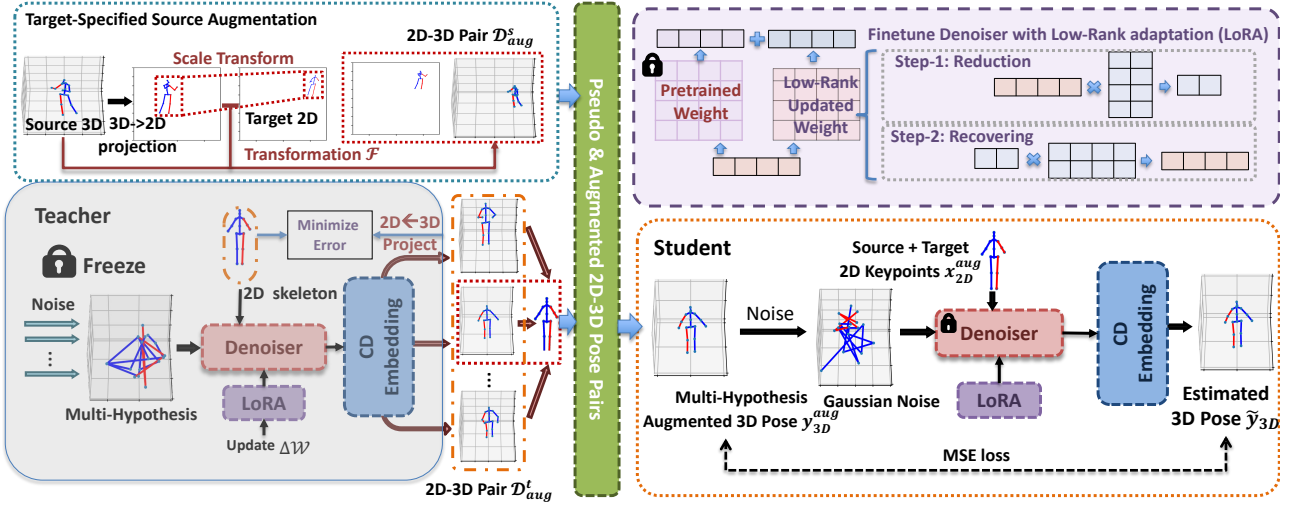


**Figure 2: The PoSynDA Framework.** Augmented source 2D-3D pairs,  $\mathcal{D}_{aug}^s$ , are derived through scale transformations on 2D skeletons, aligning them with the target 2D skeleton scale. The teacher network, with static parameters, generates multiple 3D pose hypotheses using noise samples and target 2D skeleton conditioning. These 3D poses are then projected to 2D, with the closest projection to the target 2D skeleton being chosen as its pseudo label, represented as  $\mathcal{D}_{aug}^t$ . In the student network, these augmented pairs are processed by a denoiser with LoRA and cross-dataset embedding to train the pose estimator  $\mathcal{P}$  with parameter  $\theta$ .

Our method, PoSynDA (as shown in Figure 2), adopts a teacher-student paradigm within a diffusion model framework. Here, the denoiser acts as  $\mathcal{P}$ , converting 2D keypoints to 3D poses. Multiple 3D pose hypotheses are generated through repeated sampling Gaussian noise and lifted using denoiser  $\mathcal{P}$ , and the pose closest to the ground truth is chosen as the pseudo-label. This strategy helps provide supervision in the absence of real labels. PoSynDA further leverages 3D poses from the source domain and 2D keypoints from the target domain to create a unified dataset, effectively merging both domains. Specific estimation details and the full model structure are discussed in the following sections.

### 3.2 Target-specified Source Data Augmentation

3D human pose estimation (3D HPE) is often challenged by domain shift due to differences in camera intrinsic and extrinsic parameters across datasets. To overcome this issue and improve the performance of the target dataset, we propose a target-specified source data augmentation strategy. By utilizing known camera parameters of the target dataset, we employ a 3D imaging algorithm to adapt the source data’s 3D labels to the target domain. The focus of this scheme is to minimize the impact of scale and position variations, which can be detrimental during domain adaptation.

Consider a 3D pose from the source domain dataset  $\mathcal{D}_s$ , centered at the origin  $[0, 0, 0]$ , and a 2D pose from the target domain  $\mathcal{D}_t$ . Leveraging methods from previous work [4], we randomly sample a pose pair  $(\mathbf{y}_{3D}^s, \mathbf{x}_{2D}^t)$  to approximate the target domain’s scale and position distribution using Monte Carlo techniques [21]. A transformation function  $\mathcal{F}$  is then applied to convert the source 3D pose to the 2D target domain, as follows:

$$\mathcal{D}_{aug}^s = \mathcal{F}(\mathbf{x}_{2D}^t, \mathbf{y}_{3D}^s) \quad (3)$$

Here,  $\mathcal{D}_{aug}^s$  signifies the transformed 3D pose aligned with the target domain’s distribution. A comprehensive description of the

transformation function  $\mathcal{F}$  is found in [4]. By performing this target-specified source data augmentation, we effectively bridge the gap between the source and target domains. This not only enhances the adaptability of the model but also leads to improved 3D human pose estimation performance across diverse conditions.

### 3.3 Multi-hypothesis Domain Adaptation

**Pose Synthesis.** 3D human pose estimation is complex due to depth ambiguity and self-occlusion, where multiple valid 3D solutions might correspond to a single 2D pose. To address this, our method synthesizes multiple plausible 3D poses, selecting the most likely one to represent the target. This probabilistic approach compensates for limited diversity in the target domain and lack of labeled data by utilizing multiple hypotheses to approximate the 3D pose distribution, adopting the best-matching pose as a pseudo-label.

In our 2D-to-3D lifting model, the generation of multiple hypotheses is achieved by repeated sampling of noise from a standard Gaussian distribution. The number of hypotheses, denoted as  $H$ , balances accuracy and computational efficiency, increasing hypothesis space coverage and pose diversity as  $H$  grows.

**Teacher-Student Paradigm.** We utilize a teacher-student learning paradigm, where both networks share identical weights but perform different roles. The teacher generates hypotheses and pseudo-labels without updating during training, while the student uses pseudo-labels to adjust its parameters.

- **Teacher Network.** The input 2D keypoints are transformed into a Gaussian distribution by gradually introducing noise. Subsequently, noise  $\epsilon \sim \mathcal{N}(0, \mathbf{I})$  is sampled to restore the 3D pose via a denoiser. By sampling  $H$  noises, we derive  $H$  different poses, denoted by  $\tilde{\mathbf{y}}_{0:H}$  for each frame, which are then projected into the 2D camera plane. The pseudo-label is determined by calculating the error between these projections and the original 2D keypoints  $\mathbf{x}_{2D}^t$ , selecting the

hypothesis with the minimum error as the pseudo-label:

$$h' = \arg \min_{h \in [0, H]} \|\mathcal{G}(\tilde{\mathbf{y}}_h) - \mathbf{x}_{2D}^t\|_2, \quad (4)$$

$$\tilde{\mathbf{y}}_{3D} = \tilde{\mathbf{y}}_{h'}, \quad (5)$$

where  $\mathcal{G}$  is the projection function, and  $\tilde{\mathbf{y}}_{3D}$  is the pseudo-label. The teacher focuses solely on hypothesis generation and pseudo-label determination without participating in gradient computation.

- **Student Network.** The student learns from both augmented source data  $\mathcal{D}_{aug}^s$  (from Sec. 3.2) and target data  $\mathcal{D}_{aug}^t$  obtained by the teacher. Unlike the teacher's multi-hypothesis approach, the student generates only a single 3D pose, signified by setting  $H$  to 1. After each student updates using  $\mathcal{D}_{aug}$ , the corresponding parameters are synchronized back to the teacher, maintaining coherence throughout the learning process.

This coordinated approach is detailed in Algorithm 1, encapsulating our multi-hypothesis domain adaptation method. By leveraging both the teacher and student networks, it offers an efficient and robust solution to the challenges of 3D human pose estimation, particularly in cases with limited target domain diversity.

### 3.4 Model Structure

The PoSynDA framework is designed around the diffusion model, consisting of a denoiser, LoRA (low-rank adaptation) module, and cross-dataset embedding components. These are depicted in Fig. 2. In this section, we will elucidate the diffusion model's underlying principles and describe each component in detail.

**Diffusion Model.** The Denoising Diffusion Probabilistic Model (DDPM) [26] serves as the core of the generative model, comprising two main processes. Firstly, a diffusion process progressively introduces Gaussian noise to the data. Secondly, a denoising process rebuilds the data from this noise utilizing a denoiser. Through iterative noise addition and denoising, the neural network (NN) learns to transform any Gaussian noise into the target data distribution.

Consider the target data  $\mathbf{y}_0$ . The forward process  $q$  gradually incorporates Gaussian noise,  $\epsilon$ , with a variance of  $\beta_e \in [0, 1]$  at each time step  $e$ . This leads from  $\mathbf{y}_1$  to  $\mathbf{y}_E$  as follows:

$$q(\mathbf{y}_e | \mathbf{y}_{e-1}) = \mathcal{N}(\mathbf{y}_e; \sqrt{1 - \beta_e} \mathbf{y}_{e-1}, \beta_e \mathbf{I}), \quad (6)$$

Leveraging the Markov chain property,  $\mathbf{y}_e$  in equation 6 can be directly sampled, conditioned solely on  $\mathbf{y}_0$ , as:

$$q(\mathbf{y}_e | \mathbf{y}_0) = \mathcal{N}(\mathbf{y}_e; \sqrt{\bar{\alpha}_e} \mathbf{y}_0, (1 - \bar{\alpha}_e) \mathbf{I}), \quad (7)$$

where  $\alpha_e = 1 - \beta_e$  and  $\bar{\alpha}_e = \prod_{s=1}^e \alpha_s$ . For 3D human pose estimation, the noisy 3D pose  $\mathbf{y}_e$  is fed to a denoiser  $\mathcal{P}$ , conditioned on 2D keypoints  $\mathbf{x}_{2D}$  and time step  $e$ , to reconstruct the noise-free 3D pose  $\tilde{\mathbf{y}}_0$ :

$$\tilde{\mathbf{y}}_0 = \mathcal{P}(\mathbf{x}_{2D}, \mathbf{y}_e, e). \quad (8)$$

where  $\tilde{\mathbf{y}}_0$  represents the estimated pose  $\tilde{\mathbf{y}}_{3D}$ . The denoising network is guided by a simple MSE loss:

$$\mathcal{L} = \|\mathbf{y}_0 - \tilde{\mathbf{y}}_0\|_2. \quad (9)$$

---

#### Algorithm 1: Domain adaptation training and inference algorithm

---

**Input:** Source domain  $\mathcal{D}_s = (\mathbf{x}_{2D}^s, \mathbf{y}_{3D}^s)$ , Target domain  $\mathcal{D}_t = (\mathbf{x}_{2D}^t)$ , 3D Pose Estimator  $\mathcal{P}$  with parameter  $\theta$  initialized with  $\theta_s$  trained on  $\mathcal{D}_s$ , Number of hypotheses  $H$ , Projection function  $\mathcal{G}$ , Loss function  $\mathcal{L}$ , learning rate  $\eta$

**Output:** Estimated pose  $\tilde{\mathbf{y}}_{3D}^t$  of target domain

---

```

1 Training:
2 while  $\theta$  has not converged do
3   /* sampling batch data from datasets */
4   Sample a batch from  $\mathcal{D}^t = \{(\mathbf{x}_{2D}^t)\}$ 
5   Sample a batch from  $\mathcal{D}^s = \{(\mathbf{x}_{2D}^s, \mathbf{y}_{3D}^s)\}$ 
6   Augment the source data  $\mathcal{D}_{aug}^s = \mathcal{F}(\mathbf{x}_{2D}^t, \mathbf{y}_{3D}^s)$  derived
   by Eq. 3
7   /* computing pseudo label for target data */
8   freeze Teacher  $\mathcal{P}$ 
9   for  $h \leftarrow 0$  to  $H$  do
10    sample noise  $\epsilon \sim \mathcal{N}(0, \mathbf{I})$ 
11     $\tilde{\mathbf{y}}_h = \mathcal{P}(\mathbf{x}_{2D}^t, \epsilon)$ 
12     $\tilde{\mathbf{y}}_{3D} = \tilde{\mathbf{y}}_{h'}$ ,  $h' = \arg \min_{h \in [0, H]} \|\mathcal{G}(\tilde{\mathbf{y}}_h) - \mathbf{x}_{2D}^t\|_2$ 
13     $\mathcal{D}_{aug}^t = \{(\mathbf{x}_{2D}^t, \tilde{\mathbf{y}}_{3D})\}$ 
14    /* training the student estimator  $\mathcal{P}$  */
15     $\mathcal{D}_{aug} = \text{concat}(\mathcal{D}_{aug}^s, \mathcal{D}_{aug}^t) = \{(\mathbf{x}_{2D}^{aug}, \mathbf{y}_{3D}^{aug})\}$ 
16    Sample noise  $\epsilon \sim \mathcal{N}(0, \mathbf{I})$  and forward
17    Compute the loss and gradients by Eq. 2
18    Updating  $\theta$  using Adam with
    $\theta \leftarrow \theta - \eta \nabla_{\theta} \mathcal{L}_{\mathcal{P}}(\mathcal{P}(\mathbf{x}_{2D}^{aug}, \epsilon), \mathbf{y}_{3D}^{aug})$ 
19    Update Teacher and Student  $\mathcal{P}$  with  $\theta$ 
20 Inference:
21 freeze  $\mathcal{P}$ 
22 sample noise  $\epsilon \sim \mathcal{N}(0, \mathbf{I})$ 
23  $\tilde{\mathbf{y}}_{3D}^t = \mathcal{P}(\mathbf{x}_{2D}^t, \epsilon)$ 

```

---

To create  $H$  hypotheses  $\tilde{\mathbf{y}}_{0:H,0}$  in the target domain, we repeatedly sample from a Gaussian distribution, utilizing the concatenation of 3D Gaussian noise  $\tilde{\mathbf{y}}_{0:H,e}$  and  $\mathbf{x}_{2D}^t$  as inputs for the denoiser  $\mathcal{P}$ . The optimal hypothesis is selected by choosing the estimated target pose with the minimal 2D projection error, as described in Eq. 5. This elegant formulation underpins the robustness and efficiency of our approach to 3D human pose estimation, artfully handling both the diffusion and denoising processes.

**Denoiser Model.** Our method uniquely stands out by eliminating the need for designing a separate denoiser network structure, allowing seamless integration with existing 2D-to-3D human pose estimation networks. This ensures not only forward compatibility but also broad applicability across various domains. We strategically employ the cutting-edge MixSTE [66] as our denoiser, leveraging its proven effectiveness in 2D-to-3D pose estimation. Our decision reflects a carefully considered alignment with current state-of-the-art technologies, providing a robust foundation for our approach.



Method	S	MPJPE (↓)	P-MPJPE (↓)
Pavlo <i>et al.</i> [48]	Full	37.2	27.2
Cai <i>et al.</i> [3]	Full	50.6	40.2
Martinez <i>et al.</i> [43]	Full	45.5	37.1
Zhao <i>et al.</i> [69]	Full	43.8	-
Lui <i>et al.</i> [41]	Full	34.7	-
Wang <i>et al.</i> [59]	Full	25.6	-
Li <i>et al.</i> [38]	S1	50.5	-
Pavlo <i>et al.</i> [48]	S1	51.7	-
Gong <i>et al.</i> [16]	S1	56.7	-
Gholami <i>et al.</i> [15]	S1	54.2	35.6
Chai <i>et al.</i> [4]	S1	49.9	34.2
<b>Ours</b>	S1	<b>48.1</b>	<b>33.2</b>

**Table 1: Quantitative Results on H3.6M. S represents the source domain. MPJPE and P-MPJPE are used as evaluation metrics. Source: S1. Target: S5, S6, S7, S8.**

Additionally, in the experimental section, we undertake an in-depth evaluation to assess the feasibility of employing other 2D-to-3D lifting networks, such as VideoPose [48], as potential denoisers. This underscores our commitment to versatility and continuous innovation in optimizing our denoising strategy.

**Low-Rank Adaptation (LoRA).** Full fine-tuning of larger denoisers that encompasses all model parameters is often cumbersome and inefficient. In contrast, we leverage the low-rank adaptation (LoRA) technique [27] to facilitate a streamlined and cost-effective adaptation, targeting only essential components. While LoRA is originally conceived for large-scale language models within transformer blocks, we innovatively extend its application to 3D pose estimation.

In our 3D pose estimator  $\mathcal{P}$ , pre-trained on source data, we use query, key, value, and output projection matrices, represented as  $W$ . With  $W_0$  denoting a pre-trained weight matrix and  $\Delta W$  the gradient update during adaptation, the rank of the LoRA module is defined as  $r$ . The update to the weight matrix is thus constrained to a low-rank decomposition form, expressed as  $W_0 + \Delta W = W_0 + BA$ , where  $B \in \mathbb{R}^{d \times r}$ ,  $A \in \mathbb{R}^{r \times k}$ , and the rank  $r \ll \min(d, k)$ .

The LoRA method allows us to keep  $W_0$  fixed while training the low-rank components  $A$  and  $B$ , thus formulating the forward pass of projection as:

$$p = W_0 x + \Delta W x = W_0 x + BAx, \quad (10)$$

Here,  $p$  symbolizes the resultant hidden state, and  $x$  represents the input queries or tokens. With an appropriate initialization for  $A$  and  $B$ ,  $\Delta W = BA$  is initially zero, gradually being adjusted during the adaptation phase. Our experimental setup mainly employs a rank  $r$  of 4, with variations tailored to specific conditions. This strategic utilization of LoRA emphasizes efficiency without sacrificing accuracy, demonstrating our commitment to cutting-edge adaptation strategies within the 3D pose estimation domain.

**Cross-Dataset Embedding.** Our framework introduces a targeted strategy to mitigate biases and inconsistencies in the 3D pose estimator trained on source data, aligning with research directions found in works like [2, 63]. The goal is to eliminate the disparities in scale and position that might manifest between the source

Method	CD	MPJPE (↓)	PCK (↑)	AUC (↑)
Mehta <i>et al.</i> [44]		117.6	76.5	40.8
VNect [46]		124.7	76.6	40.4
OriNet [42]		89.4	81.8	45.2
Multi Person [45]		122.2	75.2	37.8
Martinez <i>et al.</i> [43]		84.3	85.0	52.0
Zhang <i>et al.</i> [66]		57.9	94.2	63.8
Guan <i>et al.</i> [19]	✓	117.6	90.3	-
Kanazawa <i>et al.</i> [32]	✓	113.2	77.1	40.7
Wandt <i>et al.</i> [57]	✓	92.5	81.8	54.8
Ci <i>et al.</i> [13]	✓	-	74.0	36.7
Zeng <i>et al.</i> [64]	✓	-	77.6	43.8
Li <i>et al.</i> [38]	✓	99.7	81.2	46.1
Gong <i>et al.</i> [16]	✓	92.6	82.9	46.5
Gholami <i>et al.</i> [15]	✓	77.2	88.4	54.2
Chai <i>et al.</i> [4]	✓	61.3	92.1	<b>62.5</b>
<b>Ours (VideoPose)</b>	✓	60.2	93.1	58.4
<b>Ours (MixSTE)</b>	✓	<b>58.2</b>	<b>93.5</b>	59.6

**Table 2: Quantitative Results on 3DHP. CD refers to cross-domain evaluation, while no CD denotes fully supervised learning on the target domain. PCK, AUC, and MPJPE are used as evaluation metrics. Source: H3.6M. Target: 3DHP.**

and target domains, thereby creating a more versatile and robust estimator.

We fulfill this objective by incorporating an additional embedding layer at the output stage of the estimator  $\mathcal{P}$ . Specifically, during adaptation or inference, for any given condition  $x_{2D}$ , whether derived from augmented source or target data, we integrate a bias into the predicted 3D pose to produce the finalized pose estimation, symbolized as  $\mathcal{P}_\theta(x_{2D}, \epsilon)$ . The procedure is mathematically expressed as:

$$\mathcal{P}_\theta(x_{2D}, \epsilon) = \tilde{y}_{3D} + B_{\text{bias}}, \quad (11)$$

Here,  $\tilde{y}_{3D}$  denotes the intermediate output of  $\mathcal{P}$ , and  $B_{\text{bias}} \in \mathbb{R}^{3 \times J}$  is formulated through integration of designated embedding layer.

By employing this cross-dataset embedding, our model bridges the gap between the source and target domains, ensuring that the predicted poses conform more closely to the expectations of the target context. This innovation enhances the estimator’s precision and adaptability, fostering greater accuracy and reliability in 3D pose estimation across various datasets.

## 4 EXPERIMENTS

### 4.1 Datasets and Metrics

The experiments are conducted on three distinct 3D pose estimation benchmark datasets, each presenting unique characteristics and challenges: Human3.6M (H3.6M) [29], MPI-INF-3DHP (3DHP) [46], and 3DPW [56].

**Human3.6m (H3.6M).** H3.6M is recognized as one of the most extensive datasets for human pose estimation, comprising 3.6 million frames. It captures 11 subjects engaged in 15 diverse activities, such as walking, sitting, and jumping, under varying camera angles and lighting conditions. It includes detailed ground-truth annotations of skeletal joints, RGB videos, and camera calibration parameters. According to established works [15, 48], evaluations on this dataset

Method	Denoiser	Source Data Augmentation	LoRA	CD Embedding	Multi-hypothesis	MPJPE[↓]	Params (K)	FLOPs (G)
Baseline	✓	✗	✗	✗	✗	111.7	-	277.26
	✓	✓	✗	✗	✗	62.5	-	277.26
	✓	✓	✓	✗	✗	61.9	196.60	278.88
	✓	✓	✓	✓	✗	60.7	196.65	278.88
<b>Ours</b>	✓	✓	✓	✓	✓	<b>58.2</b>	<b>196.65</b>	<b>836.65</b>

**Table 3: Ablation study for each component in our method. The evaluation results are reported by MPJPE (mm), Parameters (K), and FLOPs (G). Source: H3.6M. Target: 3DHP.**

are conducted under two different setups. These setups encapsulate varying scenarios and complexities, reflecting the model’s adaptability across different domains. The Mean Per Joint Position Error (MPJPE) and Procrustes-aligned Mean Per Joint Position Error (P-MPJPE) metrics are primarily utilized for quantitative evaluation.

**MPI-INF-3DHP (3DHP).** 3DHP presents a vast and versatile dataset, including both indoor and outdoor scenes. Comprising 2,929 frames in the test set, the dataset adds a layer of complexity with its diverse backgrounds and environmental conditions. Evaluation on this dataset is multifaceted, employing metrics like MPJPE, Percentage of Correct Keypoints (PCK) with a 150mm threshold, and the Area Under the Curve (AUC) calculated across various PCK thresholds. These metrics together provide a comprehensive understanding of model performance, especially in complex real-world scenarios.

**3D People in the Wild (3DPW).** 3DPW is a unique dataset providing 3D and 2D data primarily captured outdoors. It challenges models with dynamic camera movement, variable positions, and unpredictable natural lighting. With more variability in camera positions compared to 3DHP and H3.6M, the dataset is evaluated at a capture rate of 25fps, adding temporal complexity. Methods trained on H3.6M are assessed on the 3DPW test set using MPJPE and P-MPJPE metrics. The inclusion of 3DPW facilitates the examination of the model’s robustness in uncontrolled and diverse environments.

## 4.2 Implementation Details

Our PoSynDA was implemented using PyTorch, and executed on an NVIDIA TITAN V100 GPU for optimal computational efficiency. The Adam optimizer [33] was used with a learning rate of  $6 \times 10^{-5}$ , a batch size of 4, and 1,000 timesteps. These settings were carefully tuned to ensure convergence and stable performance across the various datasets. The input sequence lengths were adapted to specific datasets, with lengths of 243 for Human3.6M, and 27 for 3DHP and 3DPW, in alignment with [67]. These values were selected to adequately represent the human motion patterns within each dataset. A stride data sampling approach was employed to prevent overlapping between sequences. Intervals were matched to the input length, maximizing the diversity of the training data and strengthening the model’s generalization capabilities.

## 4.3 Quantitative Evaluation

**H3.6M.** Table 1 presents a comparative analysis of our PoSynDA technique with previous unsupervised methodologies, focusing

Method	CD	P-MPJPE (↓)	MPJPE (↓)
Pavlo <i>et al.</i> [48]		68.0	105.0
Kocabas <i>et al.</i> [34]		51.9	82.9
Joo <i>et al.</i> [31]		55.7	-
Lin <i>et al.</i> [40]		45.6	74.7
Kocabas <i>et al.</i> [34]	✓	56.5	93.5
Gong <i>et al.</i> [16]	✓	58.5	94.1
Guan <i>et al.</i> [19]	✓	49.5	77.2
Gholami <i>et al.</i> [15]	✓	46.5	81.2
Chai <i>et al.</i> [4]	✓	55.3	87.7
<b>Ours</b>	✓	<b>45.4</b>	<b>75.5</b>

**Table 4: Quantitative Results on 3DPW. CD refers to cross-domain evaluation, while no CD denotes fully supervised learning on the target domain. P-MPJPE and MPJPE are used as evaluation metrics. Source: H3.6M. Target: 3DPW.**

on those utilizing labeled source 2D-3D pairs and target 2D keypoints, while abstaining from using ground truth 3D poses. The table’s upper section displays results utilizing the entirety of the H3.6M dataset as the source, whereas the lower section restricts the source data to subject S1. The target data spans subjects S5 to S8. By employing ground truth 2D keypoints, we ensure consistent evaluation conditions aligned with extant literature. However, it’s pertinent to mention that our evaluations vary from some prior works due to the distinction between input videos and individual frames. Impressively, PoSynDA sets new benchmarks, demonstrating enhancements of 1.8mm and 1.0mm in MPJPE and P-MPJPE, respectively, over preceding methods.

**3DHP.** The results for the 3DHP dataset, illustrated in Table 2, encompass metrics like MPJPE, PCK, and AUC, accentuating our approach’s proficiency in cross-domain evaluations. PoSynDA showcases superiority in MPJPE and PCK metrics and exhibits a competitive AUC, closely following PoseDA. When benchmarked against the previous state-of-the-art, PoSynDA achieves a commendable reduction of 3.1mm in MPJPE. Remarkably, integrating denoisers such as VideoPose or MixSTE with PoSynDA perpetuates its top-ranking performance, underscoring the model’s resilience and adaptability. **3DPW.** As shown in Table 4, our PoSynD achieves notable outperformance over prior cross-domain methods in terms of performance metrics—MPJPE and P-MPJPE— with an improvement margin of 1.7mm in MPJPE, thereby redefining performance benchmarks.

## 4.4 Qualitative Evaluation

**3D Reconstruction Visualization.** We offer a detailed qualitative analysis of the H3.6M dataset, as demonstrated in Figure 4. Our

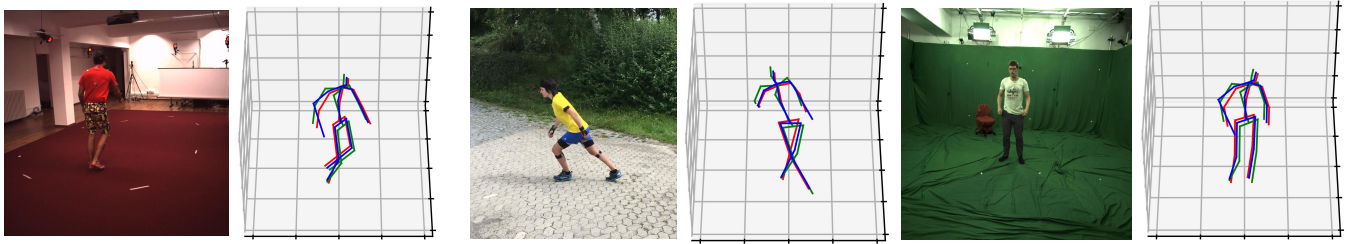


**Figure 3: Multiple hypotheses generated by our method. Each color represents a single hypothesis, and the red pose is selected as the pseudo label. These hypotheses showcase the diversity and rationality of the generated postures.**

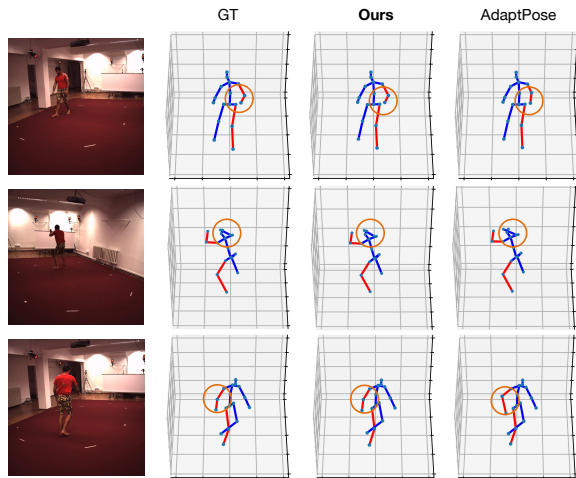


**Figure 4: Comparison of 3D estimated human pose generated by different methods. The figure displays the 3D reconstruction visualization results using our proposed method, the state-of-the-art method AdaptPose, ground truth, and the corresponding video frame from the Human3.6M dataset. The source domain is S1, and the target domains are S5, S6, S7, and S8. Our method exhibits higher accuracy and robustness in handling various actions and occlusion scenarios.**

method’s efficacy is thoroughly examined against renowned benchmarks such as AdaptPose [15]. Impressively, PoSynDA exhibits an outstanding ability to reconstruct both elementary and more intricate actions, even those obscured or occluded. This performance attests to our approach’s robustness and stability, manifesting a nuanced understanding of human pose dynamics.

**Multi-Hypothesis Generation.** Our model’s unique capacity to generate multiple plausible hypotheses is explored in Fig 3, across the diverse landscapes of the H3.6M, 3DHP, and 3DPW datasets. These visualized hypotheses do more than merely present an anatomically accurate and variegated set of potential poses. They also highlight the precise alignment between the chosen pose (emphasized in red) and the true underlying human pose. This alignment is more than a mere visual concordance; it resonates with the core principles of human movement and behavior. Hence, it not only proves the technical proficiency of PoSynDA but also

Method	MPJPE (↓)
Multi-hypothesis Method: D3DP [51]	96.5
Generative Method: GAN [17]	87.5
Ours	58.2

**Table 5: Ablation study: The table compares our method’s MPJPE performance with multi-hypothesis (D3DP) and generative (GAN) models. Source: H3.6M. Target: 3DHP.**

highlights the holistic, human-centered philosophy driving our approach.

## 4.5 Ablation Studies

**4.5.1 The Impact of Model Components.** To understand the individual components of our PoSynDA, we conducted an ablation study on H3.6M as the source and 3DHP as the target domain. We started with a baseline model that was trained as a denoiser solely on the source domain, and then systematically integrated various components to analyze their effects. This is shown in Table 3.

(1) *Baseline Analysis.* The baseline configuration displayed a pronounced domain shift, leading to subpar pose predictions. This outcome vividly sheds light on the task’s intricacy, providing a crucial context for assessing the improvements introduced later.

(2) *Source Data Augmentation.* With the implementation of the source data augmentation module, the model experienced a remarkable 44.7% improvement in MPJPE, emphasizing the pivotal role this component plays in enhancing prediction accuracy.

(3) *LoRA Integration.* The inclusion of LoRA further augmented the model’s capabilities, marking its debut success in 3D human pose estimation. This achievement represents an innovative leap, unveiling LoRA’s latent potential, and underscoring the significance of this novel integration within the framework of 3D pose analysis.

(4) *Cross-Dataset Embedding.* The incorporation of Cross-Dataset embedding, with minimal addition of only 0.05K parameters, succeeded in mitigating the bias between domains, strengthening the overall model performance. This efficient improvement illustrates the potential of nuanced optimization in enhancing the system’s efficacy.

(5) *Multi-Hypothesis Incorporation.* Although the Multi-hypothesis module increased FLOPs substantially, it fine-tuned MPJPE by 2.5mm without affecting the inference speed, as it is employed solely within the teacher network during training. This highlights

# of hypotheses	MPJPE (↓)	PCK (↑)	AUC (↑)
1	60.7	92.5	58.2
2	59.9	93.4	59.1
3	58.2	93.5	59.6
4	58.1	93.7	59.3
5	58.3	93.7	59.4
6	58.5	93.4	58.9

**Table 6: Ablation study: The table shows the impact of the number of hypotheses on the evaluation metrics MPJPE (mm), PCK (Percentage of Correct Keypoints), and AUC (Area Under the Curve). Source: H3.6M. Target: 3DHP.**

Rank	MPJPE (↓)	Params (K)	FLOPs (G)
1	62.1	49.19	835.43
2	60.4	98.34	835.83
3	59.8	147.49	836.24
4	58.2	196.65	836.65
5	58.3	245.80	837.05
6	58.1	249.95	837.46

**Table 7: Ablation study: The table presents the impact of different ranks on the diffusion model’s performance, measured by MPJPE (mm), Parameters (K), and FLOPs (G). Source: H3.6M. Target: 3DHP.**

its distinct contribution to the model, emphasizing the strategic importance of this component within the architectural design.

(6) *Comparison with Alternative Approaches.* Our analysis also included scrutiny of other pioneering techniques, such as the Multi-hypothesis Method (D3DP) and GAN-based Generation Method. As shown in Table 5, these comparative evaluations, conducted using H36M as the source and 3DHP as the target, reveal that PoSynDA’s performance surpasses both the latest state-of-the-art multi-hypothesis method, D3DP [51], and the traditional GAN approach [17]. This assessment further buttresses PoSynDA’s standing as an innovative solution in the field of 3D pose estimation.

4.5.2 *The Number of Hypotheses.* The influence of the number of hypotheses on the model’s performance was systematically examined, with H3.6M as the source domain and 3DHP as the target domain. As presented in Table 6, the experiments disclose a trend where increasing the number of hypotheses leads to an enhancement in the model’s accuracy. Nevertheless, beyond the three hypotheses, further increments fail to yield significant gains; instead, they result in fluctuations within a specific range. Considering that the FLOPs of the model increase linearly with the number of hypotheses, our experimental configuration judiciously selected three hypotheses. This choice harmonizes the dual objectives of achieving high accuracy and maintaining computational efficiency.

4.5.3 *The Structure of Diffusion Model.* The nuanced interplay between the number of timesteps and the embedding dimension of the denoiser is explored in Table 8. It reveals that augmenting both timesteps and embedding dimensions typically conduces to better performance. The zenith is reached at 1000 timesteps with an embedding dimension of 512, garnering the lowest MPJPE score of

# of timesteps	Dimension	MPJPE (↓)
100	512	59.8
500	256	59.3
500	512	59.0
1000	256	58.9
1000	512	58.2
1000	1024	58.3

**Table 8: Ablation study: The table shows the impact of different combinations of timesteps and denoiser embedding dimensions on MPJPE (Mean Per Joint Position Error). Source: H3.6M. Target: 3DHP.**

58.2mm. Remarkably, further amplifying the embedding dimension to 1024 does not reap additional benefits, thus delineating an optimal configuration at 1000 timesteps and an embedding dimension of 512.

4.5.4 *The Computational Complexity of LoRA.* The LoRA component’s computational complexity is intricately tied to its rank setting, introducing a multi-faceted trade-off between rank, computational overhead, and prediction accuracy within the realm of low-rank approximation. As Table 7 elucidates, our investigations identified a rank of 4 as a judicious selection within the LoRA architecture. This choice orchestrates an adept equilibrium between computational economy and accuracy, without sacrificing the integrity of the underlying mathematical construct.

## 5 CONCLUSION

This paper introduces a novel framework, Multi-Hypothesis Pose Synthesis Domain Adaptation (PoSynDA), for 3D human pose estimation. PoSynDA aims to generate a wide array of 3D poses in the target domain, addressing the challenge of limited diversity. PoSynDA operates using a diffusion-based structure, viewing pose estimation as a multi-step denoising diffusion process. Additionally, we propose a target-specified source augmentation scheme to create 3D pose pairs, adjusting for scale. Through evaluation of 3 benchmark datasets and comparison with state-of-the-art models, PoSynDA not only surpasses leading models but also competes with the target-domain trained model MixSTE [66]. Future exploration of PoSynDA will focus on real-world applications, such as vision perception-based interaction and video generation, to maximize the benefits of this innovative technique.

## ACKNOWLEDGMENTS

The specific contributions of Zhi-Qi Cheng in this project were supported by the Army Research Laboratory (W911NF-17-5-0003), the Air Force Research Laboratory (FA8750-19-2-0200), the U.S. Department of Commerce’s National Institute of Standards and Technology (60NANB17D156), the Intelligence Advanced Research Projects Activity (D17PC00340), and the US Department of Transportation (69A3551747111). Intel and IBM Fellowships also provided additional support for Zhi-Qi Cheng’s research work. The views and conclusions contained herein represent those of the authors and not necessarily the official policies or endorsements of the supporting agencies or the U.S. Government.



## REFERENCES

- [1] Xu Bao, Zhi-Qi Cheng, Jun-Yan He, Chenyang Li, Wangmeng Xiang, Jingdong Sun, Hanbing Liu, Wei Liu, Bin Luo, Yifeng Geng, et al. 2023. KeyPosS: Plug-and-Play Facial Landmark Detection through GPS-Inspired True-Range Multilateration. *Proceedings of the 31st ACM International Conference on Multimedia*.
- [2] Han Cai, Chuang Gan, Ligeng Zhu, and Song Han. 2020. Tinyt: Reduce activations, not trainable parameters for efficient on-device learning. *arXiv preprint arXiv:2007.11622* (2020).
- [3] Yujun Cai, Liuhaog Ge, Jun Liu, Jianfei Cai, Tat-Jen Cham, Junsong Yuan, and Nadia Magnenat Thalmann. 2019. Exploiting spatial-temporal relationships for 3d pose estimation via graph convolutional networks. In *Proceedings of the IEEE/CVF international conference on computer vision*. 2272–2281.
- [4] Wenhao Chai, Zhongyu Jiang, Jenq-Neng Hwang, and Gaoang Wang. 2023. Global Adaptation meets Local Generalization: Unsupervised Domain Adaptation for 3D Human Pose Estimation. *arXiv preprint arXiv:2303.16456* (2023).
- [5] Hanyuan Chen, Jun-Yan He, Wangmeng Xiang, Wei Liu, Zhi-Qi Cheng, Hanbing Liu, Bin Luo, Yifeng Geng, and Xuansong Xie. 2023. HDFormer: High-order Directed Transformer for 3D Human Pose Estimation. *IJCAI* (2023).
- [6] Zhi-Qi Cheng, Qi Dai, Hong Li, Jingkuan Song, Xiao Wu, and Alexander G Hauptmann. 2022. Rethinking spatial invariance of convolutional networks for object counting. In *Proceedings of the IEEE/CVF Conference on Computer Vision and Pattern Recognition*. 19638–19648.
- [7] Zhi-Qi Cheng, Qi Dai, Siyao Li, Teruko Mitamura, and Alexander Hauptmann. 2022. Gsrformer: Grounded situation recognition transformer with alternate semantic attention refinement. In *Proceedings of the 30th ACM International Conference on Multimedia*. 3272–3281.
- [8] Zhi-Qi Cheng, Jun-Xiu Li, Qi Dai, Xiao Wu, and Alexander G Hauptmann. 2019. Learning spatial awareness to improve crowd counting. In *Proceedings of the IEEE/CVF international conference on computer vision*. 6152–6161.
- [9] Zhi-Qi Cheng, Jun-Xiu Li, Qi Dai, Xiao Wu, Jun-Yan He, and Alexander G Hauptmann. 2019. Improving the Learning of Multi-column Convolutional Neural Network for Crowd Counting. In *Proceedings of the 27th ACM International Conference on Multimedia*. 1897–1906.
- [10] Zhi-Qi Cheng, Yang Liu, Xiao Wu, and Xian-Sheng Hua. 2016. Video ecommerce: Towards online video advertising. In *Proceedings of the 24th ACM international conference on Multimedia*. 1365–1374.
- [11] Zhi-Qi Cheng, Xiao Wu, Yang Liu, and Xian-Sheng Hua. 2017. Video ecommerce++: Toward large scale online video advertising. *IEEE transactions on multimedia* 19, 6 (2017), 1170–1183.
- [12] Zhi-Qi Cheng, Xiao Wu, Yang Liu, and Xian-Sheng Hua. 2017. Video2shop: Exact matching clothes in videos to online shopping images. In *Proceedings of the IEEE conference on computer vision and pattern recognition*. 4048–4056.
- [13] Hai Ci, Chunyu Wang, Xiaoxuan Ma, and Yizhou Wang. 2019. Optimizing network structure for 3d human pose estimation. In *Proceedings of the IEEE/CVF international conference on computer vision*. 2262–2271.
- [14] Alexey Dosovitskiy, Lucas Beyer, Alexander Kolesnikov, Dirk Weissenborn, Xiuhua Zhai, Thomas Unterthiner, Mostafa Dehghani, Matthias Minderer, Georg Heigold, Sylvain Gelly, et al. 2020. An image is worth 16x16 words: Transformers for image recognition at scale. *arXiv preprint arXiv:2010.11929* (2020).
- [15] Mohsen Gholami, Bastian Wandt, Helge Rhodin, Rabab Ward, and Z Jane Wang. 2022. AdaptPose: Cross-Dataset Adaptation for 3D Human Pose Estimation by Learnable Motion Generation. In *Proceedings of the IEEE/CVF Conference on Computer Vision and Pattern Recognition*. 13075–13085.
- [16] Kehong Gong, Jianfeng Zhang, and Jiashi Feng. 2021. Poseaug: A differentiable pose augmentation framework for 3d human pose estimation. In *Proceedings of the IEEE/CVF conference on computer vision and pattern recognition*. 8575–8584.
- [17] Ian Goodfellow, Jean Pouget-Abadie, Mehdi Mirza, Bing Xu, David Warde-Farley, Sherjil Ozair, Aaron Courville, and Yoshua Bengio. 2014. Generative adversarial nets. *Advances in neural information processing systems* 27 (2014).
- [18] Shanyan Guan, Jingwei Xu, Yunbo Wang, Bingbing Ni, and Xiaokang Yang. 2021. Bilevel Online Adaptation for Out-of-Domain Human Mesh Reconstruction. In *IEEE Conference on Computer Vision and Pattern Recognition (CVPR)*. 10472–10481.
- [19] Shanyan Guan, Jingwei Xu, Yunbo Wang, Bingbing Ni, and Xiaokang Yang. 2021. Bilevel online adaptation for out-of-domain human mesh reconstruction. In *Proceedings of the IEEE/CVF Conference on Computer Vision and Pattern Recognition*. 10472–10481.
- [20] Kai Han, An Xiao, Enhua Wu, Jianyuan Guo, Chunjing Xu, and Yunhe Wang. 2021. Transformer in transformer. *Advances in Neural Information Processing Systems* 34 (2021), 15908–15919.
- [21] W Keith Hastings. 1970. Monte Carlo sampling methods using Markov chains and their applications. (1970).
- [22] Alexander Hauptmann, Lijun Yu, Wenhe Liu, Yijun Qian, Zhiqi Cheng, Liangke Gui, et al. 2023. Robust Automatic Detection of Traffic Activity. (2023).
- [23] Jun-Yan He, Zhi-Qi Cheng, Chenyang Li, Wangmeng Xiang, Binghui Chen, Bin Luo, Yifeng Geng, and Xuansong Xie. 2023. DAMO-StreamNet: Optimizing Streaming Perception in Autonomous Driving. *arXiv preprint arXiv:2303.17144* (2023).
- [24] Jun-Yan He, Xiao Wu, Zhi-Qi Cheng, Zhaoquan Yuan, and Yu-Gang Jiang. 2021. DB-LSTM: Densely-connected Bi-directional LSTM for human action recognition. *Neurocomputing* 444 (2021), 319–331.
- [25] Shuting He, Hao Luo, Pichao Wang, Fan Wang, Hao Li, and Wei Jiang. 2021. Transreid: Transformer-based object re-identification. In *Proceedings of the IEEE/CVF international conference on computer vision*. 15013–15022.
- [26] Jonathan Ho, Ajay Jain, and Pieter Abbeel. 2020. Denoising diffusion probabilistic models. *Advances in neural information processing systems* 33 (2020), 6840–6851.
- [27] Edward J Hu, Yelong Shen, Phillip Wallis, Zeyuan Allen-Zhu, Yuanzhi Li, Shean Wang, Lu Wang, and Weizhu Chen. 2021. Lora: Low-rank adaptation of large language models. *arXiv preprint arXiv:2106.09685* (2021).
- [28] Siyu Huang, Haoyi Xiong, Zhi-Qi Cheng, Qingzhong Wang, Xingran Zhou, Bihan Wen, Jun Huang, and Dejing Dou. 2021. Generating Person Images with Appearance-aware Pose Stylizer. In *29th International Joint Conference on Artificial Intelligence*. International Joint Conferences on Artificial Intelligence, 623–629.
- [29] Catalin Ionescu, Dragos Papava, Vlad Olaru, and Cristian Sminchisescu. 2014. Human3.6M: Large Scale Datasets and Predictive Methods for 3D Human Sensing in Natural Environments. *IEEE Trans. Pattern Anal. Mach. Intell.* 36, 7 (2014), 1325–1339.
- [30] Ehsan Jahangiri and Alan L Yuille. 2017. Generating multiple diverse hypotheses for human 3d pose consistent with 2d joint detections. In *Proceedings of the IEEE International Conference on Computer Vision Workshops*. 805–814.
- [31] Hanbyul Joo, Natalia Neverova, and Andrea Vedaldi. 2021. Exemplar fine-tuning for 3d human model fitting towards in-the-wild 3d human pose estimation. In *2021 International Conference on 3D Vision (3DV)*. IEEE, 42–52.
- [32] Angjoo Kanazawa, Michael J Black, David W Jacobs, and Jitendra Malik. 2018. End-to-end recovery of human shape and pose. In *Proceedings of the IEEE conference on computer vision and pattern recognition*. 7122–7131.
- [33] Diederik P Kingma and Jimmy Ba. 2014. Adam: A method for stochastic optimization. *arXiv preprint arXiv:1412.6980* (2014).
- [34] Muhammed Kocabas, Nikos Athanasiou, and Michael J Black. 2020. Vibe: Video inference for human body pose and shape estimation. In *Proceedings of the IEEE/CVF conference on computer vision and pattern recognition*. 5253–5263.
- [35] Jin-Peng Lan, Zhi-Qi Cheng, Jun-Yan He, Chenyang Li, Bin Luo, Xu Bao, Wangmeng Xiang, Yifeng Geng, and Xuansong Xie. 2023. Procontext: Exploring progressive context transformer for tracking. In *IEEE International Conference on Acoustics, Speech and Signal Processing*. IEEE, 1–5.
- [36] Chenyang Li, Zhi-Qi Cheng, Jun-Yan He, Pengyu Li, Bin Luo, Hanyuan Chen, Yifeng Geng, Jin-Peng Lan, and Xuansong Xie. 2023. Longshortnet: Exploring temporal and semantic features fusion in streaming perception. In *IEEE International Conference on Acoustics, Speech and Signal Processing*. IEEE, 1–5.
- [37] Sijin Li and Antoni B Chan. 2015. 3d human pose estimation from monocular images with deep convolutional neural network. In *Computer Vision—ACCV 2014: 12th Asian Conference on Computer Vision, Singapore, Singapore, November 1-5, 2014, Revised Selected Papers, Part II 12*. Springer, 332–347.
- [38] Shichao Li, Lei Ke, Kevin Pratama, Yu-Wing Tai, Chi-Keung Tang, and Kwang-Ting Cheng. 2020. Cascaded deep monocular 3d human pose estimation with evolutionary training data. In *Proceedings of the IEEE/CVF conference on computer vision and pattern recognition*. 6173–6183.
- [39] Wenhao Li, Hong Liu, Hao Tang, Pichao Wang, and Luc Van Gool. 2022. Mh-former: Multi-hypothesis transformer for 3d human pose estimation. In *Proceedings of the IEEE/CVF Conference on Computer Vision and Pattern Recognition*. 13147–13156.
- [40] Kevin Lin, Lijuan Wang, and Zicheng Liu. 2021. Mesh graphormer. In *Proceedings of the IEEE/CVF international conference on computer vision*. 12939–12948.
- [41] Ruixu Liu, Ju Shen, He Wang, Chen Chen, Sen-ching Cheung, and Vijayan Asari. 2020. Attention mechanism exploits temporal contexts: Real-time 3d human pose reconstruction. In *Proceedings of the IEEE/CVF Conference on Computer Vision and Pattern Recognition*. 5064–5073.
- [42] Chenxu Luo, Xiao Chu, and Alan Yuille. 2018. Orinet: A fully convolutional network for 3d human pose estimation. *arXiv preprint arXiv:1811.04989* (2018).
- [43] Julieta Martinez, Rayat Hossain, Javier Romero, and James J Little. 2017. A simple yet effective baseline for 3d human pose estimation. In *Proceedings of the IEEE international conference on computer vision*. 2640–2649.
- [44] Dushyant Mehta, Helge Rhodin, Dan Casas, Pascal Fua, Oleksandr Sotnychenko, Weipeng Xu, and Christian Theobalt. 2017. Monocular 3d human pose estimation in the wild using improved cnn supervision. In *2017 international conference on 3D vision (3DV)*. IEEE, 506–516.
- [45] Dushyant Mehta, Oleksandr Sotnychenko, Franziska Mueller, Weipeng Xu, Srinath Sridhar, Gerard Pons-Moll, and Christian Theobalt. 2018. Single-shot multi-person 3d pose estimation from monocular rgb. In *2018 International Conference on 3D Vision (3DV)*. IEEE, 120–130.
- [46] Dushyant Mehta, Srinath Sridhar, Oleksandr Sotnychenko, Helge Rhodin, Mohammad Shafiee, Hans-Peter Seidel, Weipeng Xu, Dan Casas, and Christian Theobalt. 2017. Vnect: Real-time 3d human pose estimation with a single rgb camera. *Acm transactions on graphics (tog)* 36, 4 (2017), 1–14.
- [47] Phuong Anh Nguyen, Qing Li, Zhi-Qi Cheng, Yi-Jie Lu, Hao Zhang, Xiao Wu, and Chong-Wah Ngo. 2017. Vireo@ TRECVID 2017: Video-to-text, ad-hoc video search and video hyperlinking. (2017).

- [48] Dario Pavlo, Christoph Feichtenhofer, David Grangier, and Michael Auli. 2019. 3d human pose estimation in video with temporal convolutions and semi-supervised training. In *Proceedings of the IEEE/CVF Conference on Computer Vision and Pattern Recognition*. 7753–7762.
- [49] Ben Poole, Ajay Jain, Jonathan T. Barron, and Ben Mildenhall. 2022. DreamFusion: Text-to-3D using 2D Diffusion. *arXiv* (2022).
- [50] Grégory Rogez and Cordelia Schmid. 2016. MoCap-guided Data Augmentation for 3D Pose Estimation in the Wild. In *Advances in Neural Information Processing Systems (NeurIPS)*, Daniel D. Lee, Masashi Sugiyama, Ulrike von Luxburg, Isabelle Guyon, and Roman Garnett (Eds.), 3108–3116.
- [51] Wenkang Shan, Zhenhua Liu, Xinfeng Zhang, Zhao Wang, Kai Han, Shanshe Wang, Siwei Ma, and Wen Gao. 2023. Diffusion-Based 3D Human Pose Estimation with Multi-Hypothesis Aggregation. *arXiv preprint arXiv:2303.11579* (2023).
- [52] Guang-Lu Sun, Zhi-Qi Cheng, Xiao Wu, and Qiang Peng. 2018. Personalized clothing recommendation combining user social circle and fashion style consistency. *Multimedia Tools and Applications* 77 (2018), 17731–17754.
- [53] Xiao Sun, Jiayang Shang, Shuang Liang, and Yichen Wei. 2017. Compositional human pose regression. In *Proceedings of the IEEE international conference on computer vision*. 2602–2611.
- [54] Guy Tevet, Sigal Raab, Brian Gordon, Yonatan Shafir, Amit H Bermano, and Daniel Cohen-Or. 2022. Human Motion Diffusion Model. *arXiv preprint arXiv:2209.14916* (2022).
- [55] Shuyuan Tu, Qi Dai, Zuxuan Wu, Zhi-Qi Cheng, Han Hu, and Yu-Gang Jiang. 2023. Implicit temporal modeling with learnable alignment for video recognition. *arXiv preprint arXiv:2304.10465* (2023).
- [56] Timo Von Marcard, Roberto Henschel, Michael J Black, Bodo Rosenhahn, and Gerard Pons-Moll. 2018. Recovering accurate 3d human pose in the wild using imus and a moving camera. In *Proceedings of the European conference on computer vision (ECCV)*. 601–617.
- [57] Bastian Wandt and Bodo Rosenhahn. 2019. Repnet: Weakly supervised training of an adversarial reprojection network for 3d human pose estimation. In *Proceedings of the IEEE/CVF conference on computer vision and pattern recognition*. 7782–7791.
- [58] Jinbao Wang, Shujie Tan, Xiantong Zhen, Shuo Xu, Feng Zheng, Zhenyu He, and Ling Shao. 2021. Deep 3D human pose estimation: A review. *Computer Vision and Image Understanding* 210 (2021), 103225.
- [59] Jingbo Wang, Sijie Yan, Yuanjun Xiong, and Dahua Lin. 2020. Motion guided 3d pose estimation from videos. In *Computer Vision–ECCV 2020: 16th European Conference, Glasgow, UK, August 23–28, 2020, Proceedings, Part XIII* 16. Springer, 764–780.
- [60] Wangmeng Xiang, Chao Li, Biao Wang, Xihan Wei, Xian-Sheng Hua, and Lei Zhang. 2022. Spatiotemporal self-attention modeling with temporal patch shift for action recognition. In *European Conference on Computer Vision*. Springer, 627–644.
- [61] Wangmeng Xiang, Chao Li, Yuxuan Zhou, Biao Wang, and Lei Zhang. 2023. Language supervised training for skeleton-based action recognition. *Proceedings of the IEEE/CVF International Conference on Computer Vision (ICCV)* (2023).
- [62] Jiarui Xu, Sifei Liu, Arash Vahdat, Wonmin Byeon, Xiaolong Wang, and Shalini De Mello. 2023. Open-Vocabulary Panoptic Segmentation with Text-to-Image Diffusion Models. *arXiv preprint arXiv:2303.04803* (2023).
- [63] Elad Ben Zaken, Shauli Ravfogel, and Yoav Goldberg. 2021. Bitfit: Simple parameter-efficient fine-tuning for transformer-based masked language-models. *arXiv preprint arXiv:2106.10199* (2021).
- [64] Ailing Zeng, Xiao Sun, Fuyang Huang, Minhao Liu, Qiang Xu, and Stephen Lin. 2020. Srnet: Improving generalization in 3d human pose estimation with a split-and-recombine approach. In *Computer Vision–ECCV 2020: 16th European Conference, Glasgow, UK, August 23–28, 2020, Proceedings, Part XIV* 16. Springer, 507–523.
- [65] Jianfeng Zhang, Xuecheng Nie, and Jiashi Feng. 2020. Inference Stage Optimization for Cross-scenario 3D Human Pose Estimation. In *Advances in Neural Information Processing Systems (NeurIPS)*.
- [66] Jinlu Zhang, Zhigang Tu, Jianyu Yang, Yujin Chen, and Junsong Yuan. 2022. Mixste: Seq2seq mixed spatio-temporal encoder for 3d human pose estimation in video. In *Proceedings of the IEEE/CVF Conference on Computer Vision and Pattern Recognition*. 13232–13242.
- [67] Jinlu Zhang, Zhigang Tu, Jianyu Yang, Yujin Chen, and Junsong Yuan. 2022. MixSTE: Seq2seq Mixed Spatio-Temporal Encoder for 3D Human Pose Estimation in Video. In *IEEE Conference on Computer Vision and Pattern Recognition (CVPR)*. 13222–13232.
- [68] Bo Zhao, Xiao Wu, Zhi-Qi Cheng, Hao Liu, Zequn Jie, and Jiashi Feng. 2018. Multi-view image generation from a single-view. In *Proceedings of the 26th ACM international conference on Multimedia*. 383–391.
- [69] Long Zhao, Xi Peng, Yu Tian, Mubbasir Kapadia, and Dimitris N Metaxas. 2019. Semantic graph convolutional networks for 3d human pose regression. In *Proceedings of the IEEE/CVF conference on computer vision and pattern recognition*. 3425–3435.
- [70] Ce Zheng, Sijie Zhu, Matias Mendieta, Taojiannan Yang, Chen Chen, and Zhengming Ding. 2021. 3d human pose estimation with spatial and temporal transformers. In *Proceedings of the IEEE/CVF International Conference on Computer Vision*. 11656–11665.
- [71] Xingyi Zhou, Xiao Sun, Wei Zhang, Shuang Liang, and Yichen Wei. 2016. Deep kinematic pose regression. In *Computer Vision–ECCV 2016 Workshops: Amsterdam, The Netherlands, October 8–10 and 15–16, 2016, Proceedings, Part III* 14. Springer, 186–201.
- [72] Yuxuan Zhou, Zhi-Qi Cheng, Jun-Yan He, Bin Luo, Yifeng Geng, Xuansong Xie, and Margret Keuper. 2023. Overcoming Topology Agnosticism: Enhancing Skeleton-Based Action Recognition through Redefined Skeletal Topology Awareness. *arXiv preprint arXiv:2305.11468* (2023).
- [73] Yuxuan Zhou, Chao Li, Zhi-Qi Cheng, Yifeng Geng, Xuansong Xie, and Margret Keuper. 2022. Hypergraph transformer for skeleton-based action recognition. *arXiv preprint arXiv:2211.09590* (2022).